NATIONAL HURRICANE RESEARCH PROJECT

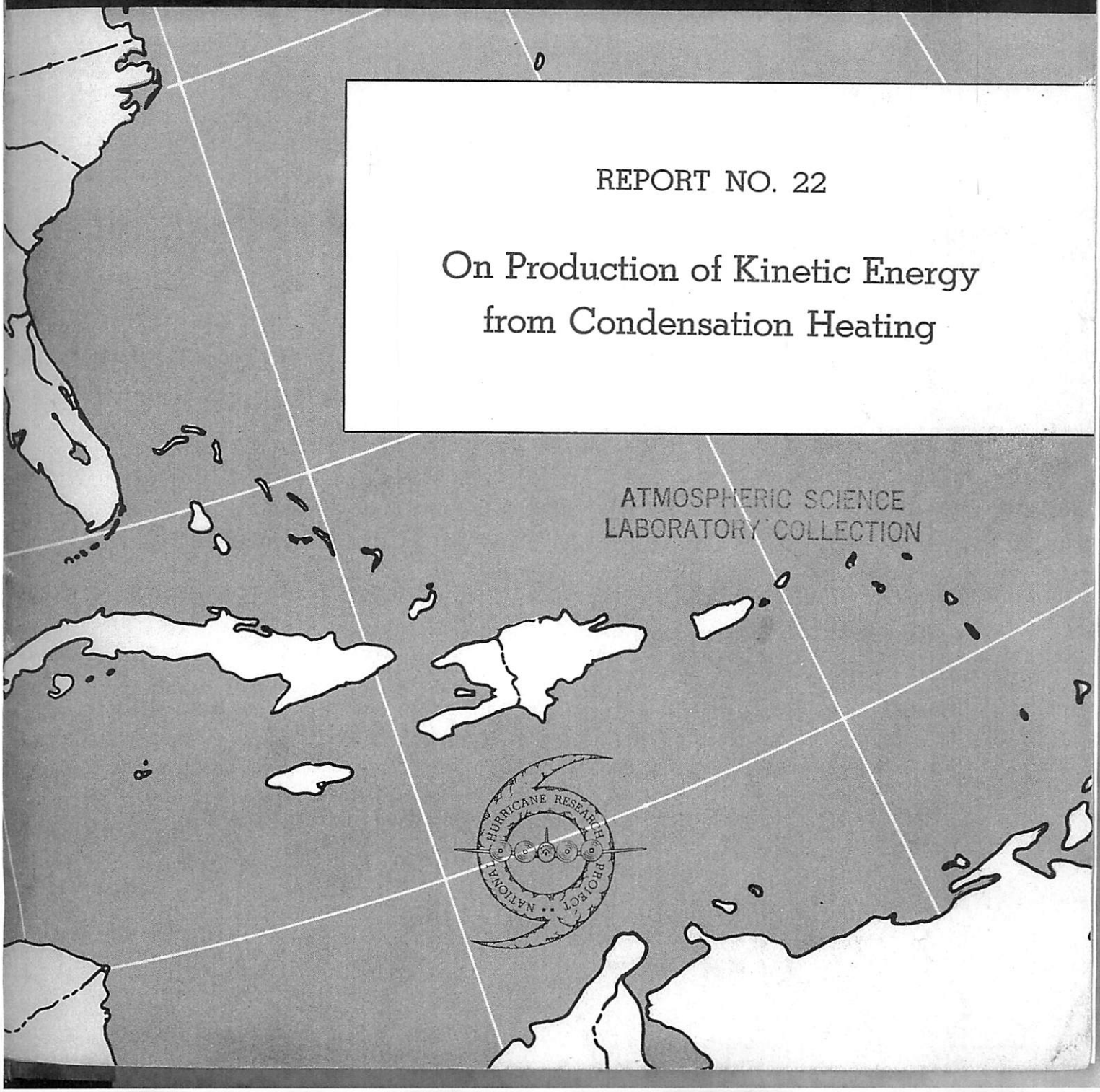

REPORT NO. 22

On Production of Kinetic Energy from Condensation Heating

U. S. DEPARTMENT OF COMMERCE
Lewis L. Strauss, Secretary
WEATHER BUREAU
F. W. Reichelderfer, Chief

NATIONAL HURRICANE RESEARCH PROJECT

REPORT NO. 22

On Production of Kinetic Energy from Condensation Heating

by
Herbert Riehl
The University of Chicago, Chicago, Ill.

Washington, D. C.
October 1958

NATIONAL HURRICANE RESEARCH PROJECT REPORTS

Reports by Weather Bureau units, contractors, and cooperators working on the hurricane problem are pre-printed in this series to facilitate immediate distribution of the information among the workers and other interested units. As this limited reproduction and distribution in this form do not constitute formal scientific publication, reference to a paper in the series should identify it as a pre-printed report.

No. 1. Objectives and basic design of the National Hurricane Research Project. March 1956.

No. 2. Numerical weather prediction of hurricane motion. July 1956.
Supplement: Error analysis of prognostic 500-mb. maps made for numerical weather prediction of hurricane motion. March 1957.

No. 3. Rainfall associated with hurricanes. July 1956.

No. 4. Some problems involved in the study of storm surges. December 1956.

No. 5. Survey of meteorological factors pertinent to reduction of loss of life and property in hurricane situations. March 1957.

No. 6. A mean atmosphere for the West Indies area. May 1957.

No. 7. An index of tide gages and tide gage records for the Atlantic and Gulf coasts of the United States. May 1957.

No. 8. Part I. Hurricanes and the sea surface temperature field.
Part II. The exchange of energy between the sea and the atmosphere in relation to hurricane behavior. June 1957.

No. 9. Seasonal variations in the frequency of North Atlantic tropical cyclones related to the general circulation. July 1957.

No. 10. Estimating central pressure of tropical cyclones from aircraft data. August 1957.

No. 11. Instrumentation of National Hurricane Research Project aircraft. August 1957.

No. 12. Studies of hurricane spiral bands as observed on radar. September 1957.

No. 13. Mean soundings for the hurricane eye. September 1957.

No. 14. On the maximum intensity of hurricanes. December 1957.

No. 15. The three-dimensional wind structure around a tropical cyclone. January 1958.

No. 16. Modification of hurricanes through cloud seeding. May 1958.

No. 17. Analysis of tropical storm Frieda, 1957. A preliminary report. June 1958.

No. 18. The use of mean layer winds as a hurricane steering mechanism. June 1958.

No. 19. Further examination of the balance of angular momentum in the mature hurricane. July 1958.

No. 20. On the energetics of the mature hurricane and other rotating wind systems. July 1958.

No. 21. Formation of tropical storms related to anomalies of the long-period mean circulation. September 1958

USCOMM-WB-DC

ON PRODUCTION OF KINETIC ENERGY FROM CONDENSATION HEATING

Herbert Riehl
The University of Chicago

[Manuscript received July 8, 1958]

ABSTRACT

Warm anticyclones extending to the high troposphere are usually regarded as "dynamic" anticyclones. In this paper a situation is presented where a warm High was of thermal origin, produced and maintained by release of latent heat of condensation. The interior of the High was filled with cloud and rain; maximum precipitable water content of the air was found in the central parts of the High.

This situation occurred over the Gulf of Mexico and the southeastern United States during September 1957. It is now known that this type of circulation occurs fairly frequently in subtropical and tropical latitudes. Therefore, the warm thermal High should be added to the types of disturbances known to exist in the atmosphere. Such a High affords simple direct means for converting latent heat energy to potential and then to kinetic energy. Calculations of the energy budget of the High showed that, over the four days analyzed, there was little export or import of heat through the boundary. A gradual increase in the intensity of the system was produced by an excess of local heat source at the ocean surface over net outgoing radiation.

The warm thermal High is associated with a "direct" mass circulation: inflow and convergence near the surface, outflow with divergence near the top. From vorticity and balanced wind considerations low pressure should develop at the surface underneath the warm High, and this took place. Thus the mass circulation was directed everywhere toward lower pressure; it released potential and produced kinetic energy. A large export of kinetic energy took place through the boundaries of the system, manifested by formation of two jet streams on its northern and eastern peripheries.

1. INTRODUCTION

A simple model of a thermal atmospheric heat engine may be summarized as follows. Given an area with heat source (radiation or condensation), air converges toward this area at low altitudes and high pressures, and it diverges from it at high altitudes and low pressures. Ascent takes place at higher temperatures than descent, hence potential energy is released. For steady state, continued heating restores the potential energy, because the heating occurs at high pressures relative to the compensatory cooling, which will be the net radiation cooling of the atmosphere at large.

Applying the theorem of conservation of potential vorticity, the inflowing current will develop cyclonic rotation and the outflowing current anticyclonic rotation. If the system is large enough so that quasi-gradient balance of forces is maintained, the pressure at the center of the heated area will be low relative to its surroundings on the horizontal plane in the layer of inflow; it will be high relative to the surroundings in the layer of outflow. The horizontal motion will be directed everywhere from high to low pressure, and this results in generation of kinetic energy. The efficiency of the heat engine in converting heat to kinetic energy may be defined as the ratio of kinetic energy produced by pressure forces to the strength of the heat source, condensation heating in the case to be considered here.

While features of the general circulation such as whole trade wind cells and the monsoons bear a resemblance to the scheme outlined, cases of simple heat engines have not been observed in the daily or secondary disturbances of the Tropics apart from hurricanes. Such circulations should exist in the Tropics where most condensation heating occurs, as counterpart to the kinetic energy releasing cyclones of middle and high latitudes. Most evidence, however, has been discouraging as brought out earlier by the writer (Riehl [7]). Even the equatorial trough zone does not have a warm core structure everywhere (Simpson [12]). Precipitation in the Tropics tends to occur in and around cold-core troughs or cyclones in the upper troposphere, while the upper anticyclones are the well known "dynamic" Highs where the high temperatures are produced by subsidence. This situation introduces considerable difficulties (cf. Riehl [10] p. 247 ff.) because all these systems are "indirect" circulations which, for genesis and maintenance, must depend on energy releases elsewhere. As yet the energy cycle maintaining such systems has remained intractable.

The increasing amount of upper-air data collected in the Tropics since the 1940's, especially the advent of rawin observations, has confirmed the predominant association of precipitation with cold-core disturbances. Occasionally, however, other types of patterns have also appeared. Some years ago the writer first published a description of a case where condensation heating may have contributed materially to the building of an upper anticyclone (Riehl and Burgner [8]). This type of association has also been suspected in other cases observed since that time, but documentation was too fragmentary to warrant detailed inquiry. It is only with expansion of the raob-rawin network over the United States in recent years, and establishment of a large number of upper-air stations around the Caribbean

Sea and Gulf of Mexico by the National Hurricane Research Project of the U.S. Weather Bureau, that a minimal amount of information has become available for quantitative evaluation of energy cycles.

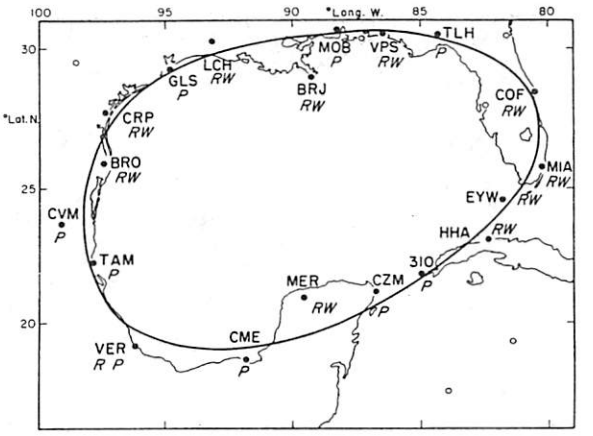

Figure 1. - Location of stations used in study; type of observations made shown with international symbols.

It is the purpose of this paper to demonstrate the existence of a simple heat engine, as described initially, for a specific situation, and then to calculate the energy transformations executed by this heat engine as well as possible. It must be emphasized that the latter objective cannot be carried out perfectly with existing data, and that therefore the present work must be regarded as no more than a first attempt to effect a transition from the qualitative to the quantitative stage in tropical weather forecasting. Nevertheless, the mere existence of the circulation to be described - as nearly a "prime mover" as one may hope to find - is believed to warrant presentation of the following case history.

2. THE WEATHER SITUATION, SEPTEMBER 15-18, 1957

Analysis of tropical circulations over the oceans has always been handicapped by lack of station networks; it has seldom been possible to obtain more than a passing and fragmentary view of any development one wished to follow. In this respect the Gulf of Mexico offers superior opportunities. While there are no weather ship stations inside this body of water, it is at least ringed by a sizable number of upper-air stations (fig. 1). The Gulf is sufficiently small that gross aspects of the weather situation over the water are fairly well described by this ring, which has a nearly elliptical shape and will be called the "Gulf ellipse."

Surface: Figures 2-22 describe the situation observed during the period September 15-18, 1957. Only 24-hour continuity is shown. At the surface we observe at first a wave disturbance in the easterlies in the eastern part of the Gulf (fig. 2); this disturbance had moved westward into this area from the Atlantic and Caribbean during the preceding day. Shortly after our map time a cyclonic center began to develop in the trough and drift north-northwestward with the prevailing tropospheric current. This center was well defined on the next day (fig. 3); it is the principal thermal cyclone of the case.

Proximity to the coast prevented further deepening of this center, but on September 17 (fig. 4) another Low appeared in the southwestern Gulf. Data over Central America confirm that this second center had been drawn northward across Central America from the equatorial trough zone of the Pacific. It

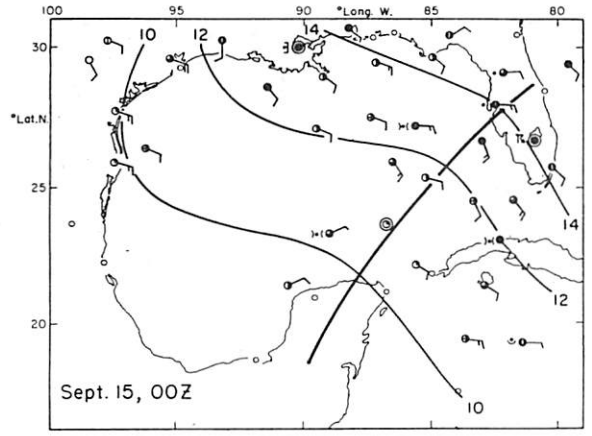

Figure 2. - 1000-mb. chart, Sept. 15, 1957, 0000 GMT. Contours in tens of feet. Heavy line denotes axis of wave trough. International weather and sky symbols used.

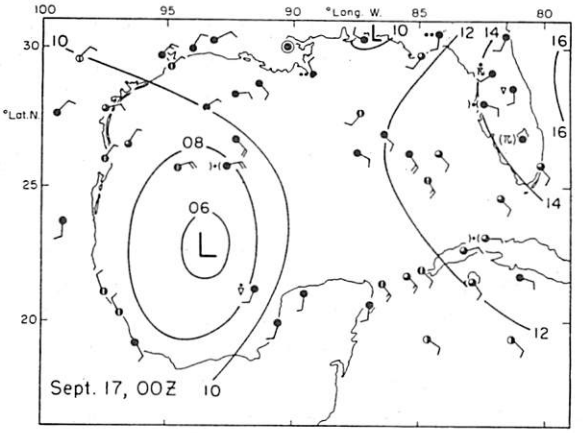

Figure 4. - 1000-mb. chart, Sept. 17, 1957, 0000 GMT.

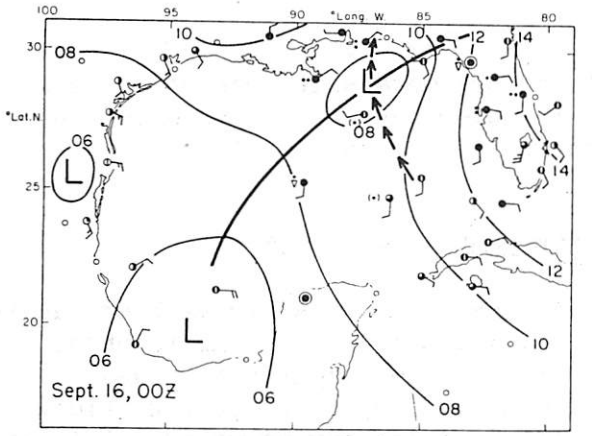

Figure 3. - 1000-mb. chart, Sept. 16, 1957, 0000 GMT.

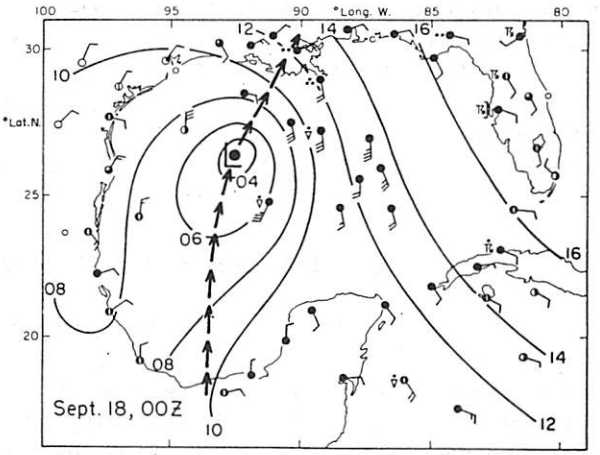

Figure 5. - 1000-mb. chart, Sept. 18, 1957, 0000 GMT.

must be regarded as a feature extraneous to the initial development of the simple heat engine over the Gulf, which was then brought in contact with it. This combination at once suggests the possibility of hurricane formation. Indeed, on September 18 (fig. 5) the center had developed into a tropical storm with strongest winds above 50 knots. The hurricane, however, failed to materialize, and the disturbance entered the coast near New Orleans as a rather weak storm.

850 mb: All upper-air observations around the Gulf have been reproduced at 850 mb. and higher levels. It must be noted that the radiosonde observations at several stations were subject to systematic errors; based on experience, these errors have been adjusted in the analysis. Initially, we observe a marked trough over the eastern Gulf (fig. 6) above the position of the surface trough line. The current passing through this trough had even larger amplitude on the preceding day, when the disturbance extended from the Bahamas across Cuba to the Caribbean. At that time the 850-mb. trough

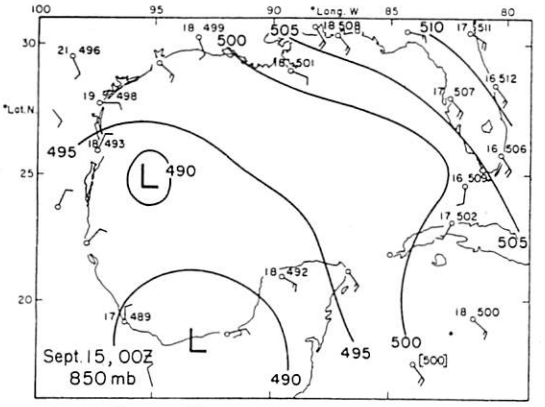

Figure 6. - 850-mb. chart, Sept. 15, 1957, 0000 GMT. Heights in tens of feet, temperatures in °C.

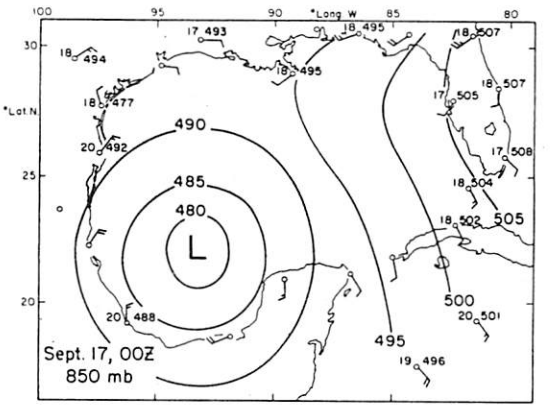

Figure 8. - 850-mb. chart, Sept. 17, 1957, 0000 GMT.

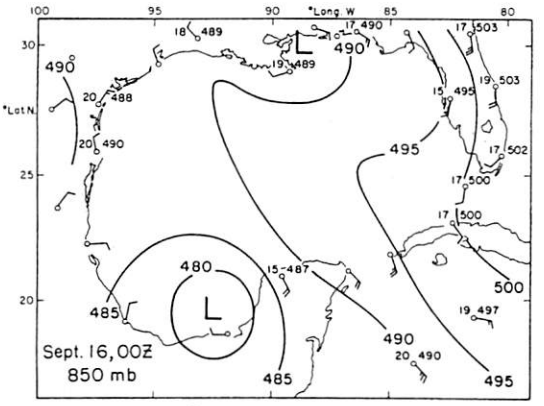

Figure 7. - 850-mb. chart, Sept. 16, 1957, 0000 GMT.

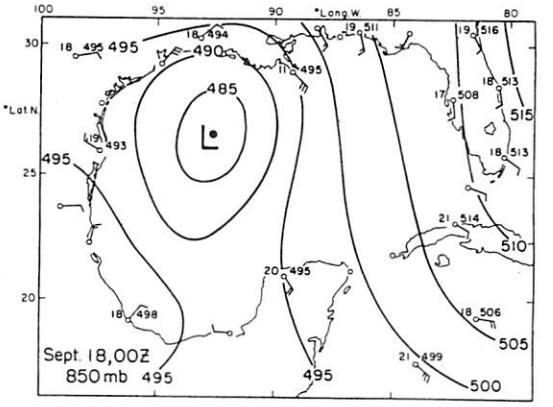

Figure 9. - 850-mb. chart, Sept. 18, 1957, 0000 GMT.

also was much better developed than the surface trough, suggesting a cold-core structure of the wave as normally encountered at low levels in the easterlies. The change from September 14 to 15 indicates that the wave structure was not steady, but that transition to a warm-core system was taking place, as evidenced also by the formation of a surface center during September 15.

Present on September 15 also was cyclonic turning of the winds over the southwestern Gulf. On the next day (fig. 7) a low pressure center clearly has entered this area, as already noted on the surface analysis. The trough in the northeastern Gulf weakened from the preceding day. As shown by the Burrwood observation (BRJ in fig. 1), the 850-mb. trough was situated will to the north of the position of the surface Low, indicating further warm-core development. The amplitude of the trough over Florida also has greatly diminished.

The map for September 17 (fig. 8) is spectacular. Strong cyclonic growth has occurred in the western Gulf as the disturbance located there came into contact with the thermal heat engine over the Gulf. In its gross features the map resembles that of June 25, 1957 when formation of a hurricane of great intensity ensued. On the last day of the series (fig. 9) the

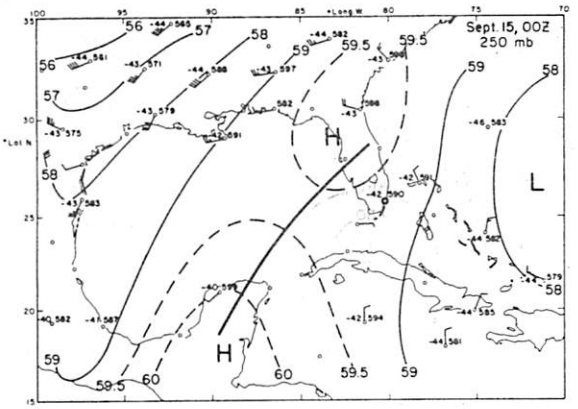

Figure 10. - 250-mb. chart, Sept.15, 1957, 0000 GMT. Contours in hundreds of feet, base 30,000 feet.

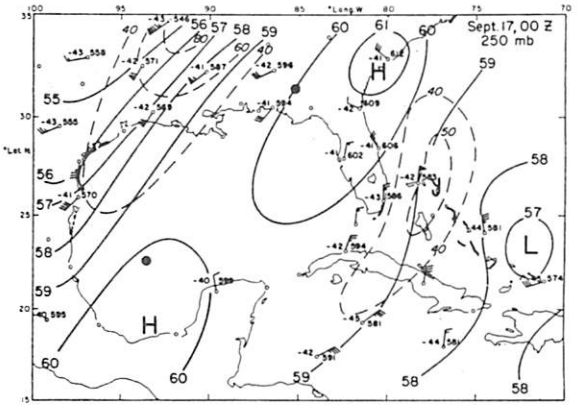

Figure 12. - 250-mb. chart, Sept.17, 1957, 0000 GMT. Includes isotachs (dashed, in knots).

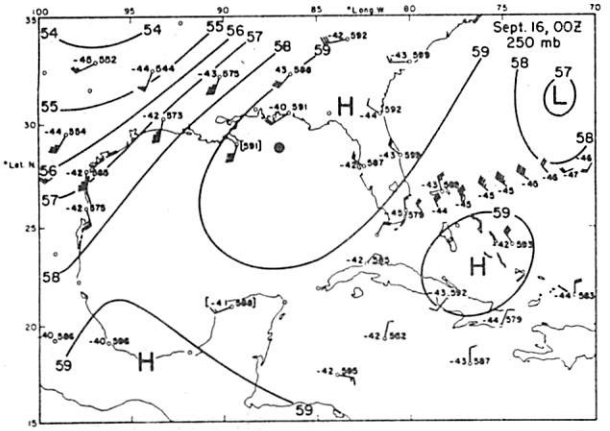

Figure 11. - 250-mb. chart, Sept.16, 1957, 0000 GMT. Heavy dot denotes surface center.

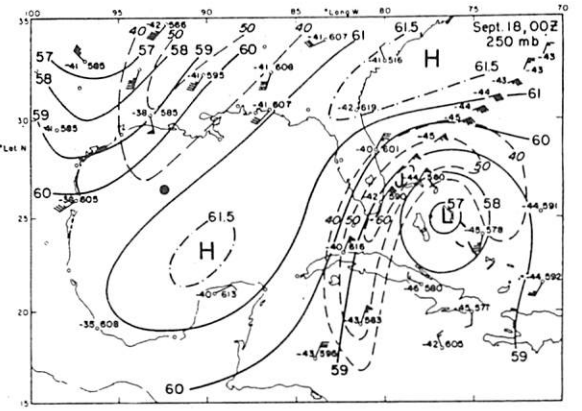

Figure 13. - 250-mb. chart, Sept.18, 1957, 0000 GMT. Includes isotachs and B-47 aircraft flight data east of Florida.

cyclone approached the northern Gulf coast under the steering influence of a strengthening Bermuda High to the east.

250 mb: The preceding charts outline the low-level circulation. As frequently emphasized by the writer (cf. Riehl [10], p. 253) the tropical troposhere tends to be divided into two portions, each with a distinct circulation regime. The transition occurs near 500 mb., where winds are often weak and confused. This was true in the present case; hence we shall omit the middle troposhere and pass on directly to the high troposhere. The level for presentation will be 250 mb., chosen because a B-47 aircraft operated by the National Hurricane Research Project

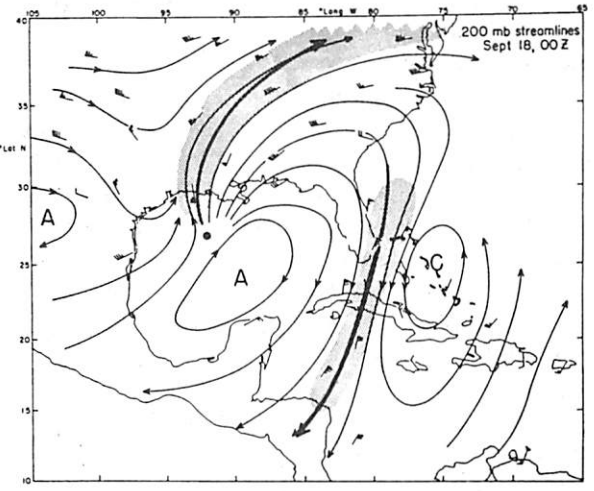

Figure 14. - Streamlines at 200 mb., Sept. 18, 1957, 0000 GMT. Area with winds above 60 knots shaded.

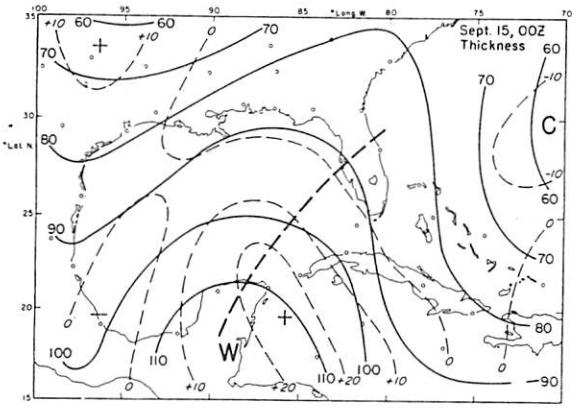

Figure 15. - Thickness 850-250 mb. (tens of feet, base 30,000 feet), Sept. 15, 1957, 0000 GMT. 24-hour thickness changes (tens of feet) dashed.

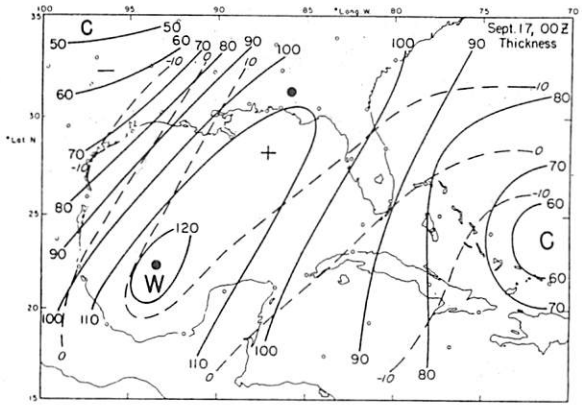

Figure 17. - Thickness 850-250 mb., Sept. 17, 1957, 0000 GMT.

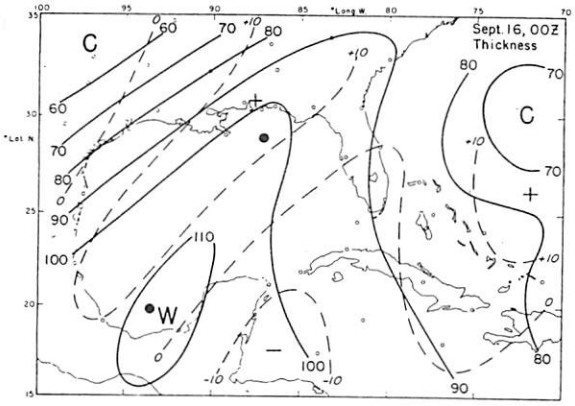

Figure 16. - Thickness 850-250 mb., Sept. 16, 1957, 0000 GMT.

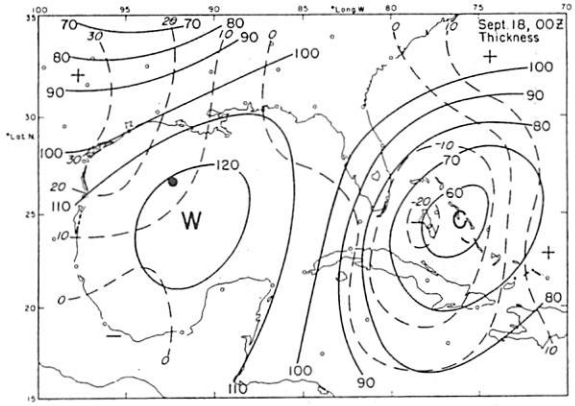

Figure 18. - Thickness 850-250 mb., Sept. 18, 1957, 0000 GMT.

was flying near this pressure surface and supplying critical information over otherwise uncharted areas.

On September 15 a ridge extending from the Yucatan peninsula to the southeastern United States was already in evidence (fig. 10). The surface trough line has also been entered. It was situated almost directly under the upper ridge after westward displacement from the area of cyclonic circulation at 250 mb. in the west central Atlantic. The map, therefore, shows the period of organization of the heat engine, brough about by relative motion of the low-level disturbance traveling under the influence of the easterlies to a position underneath the high-tropospheric ridge. Deepening in the low-level trough began shortly after the superposition took effect.

On the next day (fig. 11) the wind circulation about the upper High increased considerably. While the data do not permit precise drawing of the contours, there can be little doubt that air was crossing the 250-mb. contours toward lower pressure on both sides of the High, and that this movement represented the outflow of mass funneled upward in the convergence zone attending the surface center. Since this center with its heavy precipitation

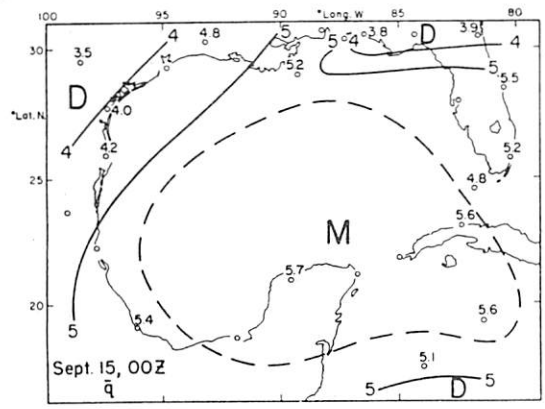

Figure 19. - Total moisture content ($g./cm.^2$), Sept. 15, 1957, 0000 GMT.

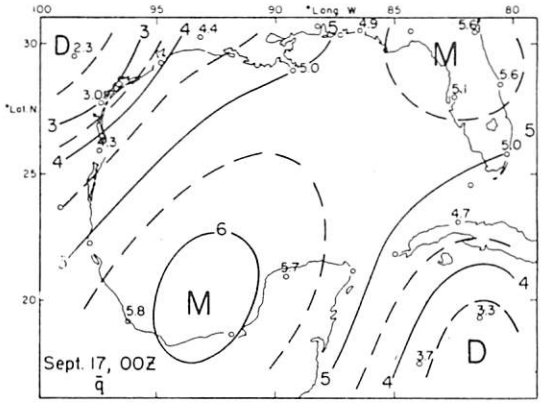

Figure 21. - Total moisture content, Sept. 17, 1957, 0000 GMT.

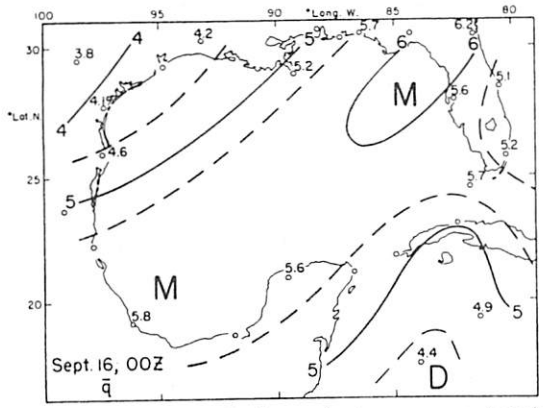

Figure 20. - Total moisture content, Sept. 16, 1957, 0000 GMT.

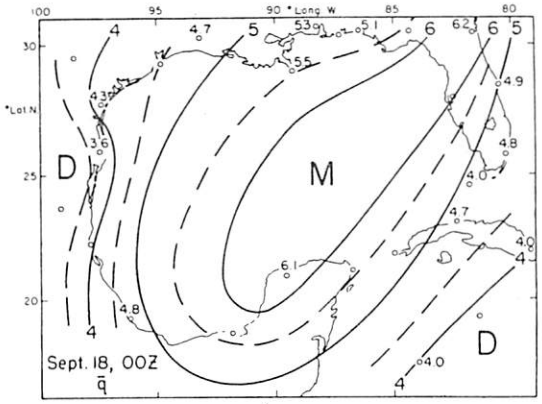

Figure 22. - Total moisture content, Sept. 18, 1957, 0000 GMT.

area was situated almost centrally underneath the upper High, the thermal heat engine was fully developed at this time.

By September 17 (fig. 12), continued building of the upper anticyclone resulted in the appearance of two jet streams which developed on eastern and western margins of the heat engine. Even more spectacular are figures 13 and 14. The cyclone in the western Gulf acted to strengthen the southwesterly jet stream, with strong movement of air toward lower pressure evident in figure 13 especially at Lake Charles (LCH). In addition, the eastern jet stream was reinforced by westward advance of a large cold Low from the Atlantic.

The thickness field for the layer 850-250 mb. (figs. 15-18) reveals a gradual increase in internal energy associated with the growth of the thermal heat engine. Both surface centers have been entered with heavy dots in the thickness charts. They were situated along the axis of warmest air, definitely establishing their warm-core nature.

Total moisture charts: Formerly, the moisture element of the radiosonde instrument was considered too unreliable to warrant computations of total precipitable water content of the air. Further, one might expect that, on account of small-scale moisture gradients in the Tropics, the total moisture determined by any particular ascent would be unrepresentative for analysis

of a station network with spacing of stations as shown in figure 1. Nevertheless, recent experimentation with total moisture charts in the tropical Atlantic and Pacific has brought out that in general the patterns are broad-scale, that they can be traced readily from map to map, and that the time sequence of total moisture at one station generally follows a regular course. For these reasons the analyses of figures 19-22 are considered quite reliable. Since a high correlation between total moisture and cloudiness and weather may be expected, the total moisture charts provide a good measure of the weather distribution over tropical areas. Previously, owing to the showery nature of rainfall and local influences over land and at coastlines, it had been difficult in many cases to obtain reliable knowledge of the location of disturbed and undisturbed areas.

After the first day, moisture gradients were strong and well organized over the Gulf area. Isolines almost paralleled the 250-mb. contours and the 850-250-mb. thickness lines. The axes of high temperature and high moisture coincided, revealing clearly that the high temperatures were derived from condensation heating. This is the final piece of evidence needed to establish the existence of a thermal heat engine. It is of more than casual interest that the moisture gradient on both sides of the wet area increased with time, indicating subsidence in the periphery. Further, since the moisture decreased from the stationary maximum over the Gulf not only toward the northwest but also toward the southeast – with low-level air motion into the Gulf from the southeast – it is evident that the deep moist layer over the Gulf was not produced by horizontal advection from the equatorial zone but by low-level convergence in the inflowing southeasterly stream. As stressed earlier by the writer (Riehl [10], pp. 51-53), dynamic features of the wind field govern the observed gradients of temperature and moisture above the mixed sub-cloud layer.

3. MASS BALANCE

While it was a rather simple task to demonstrate the existence of the heat engine qualitatively, quantitative determination of the energy transformations is difficult. The only possible approach is by means of line integrals, and for these only one line of stations is available, the Gulf ellipse of figure 1. It would be preferable to develop coordinate systems fitted with respect to the upper anticyclone, and also to place the origin of polar coordinate systems in the two cyclones. None of these things can be done unless the analyses of figures 2-22 and of other constant pressure surfaces are considered sufficiently reliable for mass flow, divergence, cross-isobar flow, etc. This is not the case, and the only quantitative use of the analyses will be determination of total energy and moisture inside the volume bounded by the ellipse.

We place a coordinate system s, n with velocity components c_s, c_n along the ellipse. The s-axis is parallel to the ellipse; cyclonic c_s is considered positive; c_n is normal to c_s and taken positive inward. Quantities

averaged around the ellipse will be denoted with a bar, deviations from such means with primes. At first we shall compute the mean circulations $\bar{c}_n$, $\bar{c}_s$ for each day. Since $\bar{c}_n$ is the mean ageostrophic indraft or outdraft, the computation is quite critical. This important component is quite small, and its integrated value around the ellipse and from the surface to the top of the circulation cell must vanish when calculated to the nearest 1/10 m.p.s. The reason for this lies in the fact that the net change of mass within the ellipse is very small percentally (one tenth of one percent of total mass), hence will be treated as zero.

Of course, $\bar{c}_n$ and $\bar{c}_s$ as such are not of great significance for the present problem because the boundary is not a special one chosen from physical considerations but from geography. The interest resides mainly in total energy fluxes; to obtain these, the transport by the mean ageostrophic circulation, possibly a large term, must nevertheless be calculable.

The top of the circulation cell is defined as the lowest pressure to which air can penetrate from the surface through buoyancy following the parcel ascent. Studies made by the Thunderstorm Project (Braham [1]) and recent work on the heat balance in the equatorial trough zone (Riehl and Malkus [11]) have shown that much of the net ascent in convective clouds takes place in cumulonimbus cores protected by surrounding cloud matter from entrainment of unsaturated air during ascent. Hence the parcel ascent really occurs; it plays a considerable role in establishing temperatures and heights of isobaric surfaces in the upper troposphere where the rising mass spreads laterally. Given the surface properties of the air and the mean vertical sounding, the top of the circulation cell can be found from a thermodynamic chart. Alternately, one can compute the vertical distribution of heat and potential energy of the atmosphere and find the pressure to which air with the observed surface properties can rise. This ascent can be represented on a diagram of $Q = gz + c_pT + Lq$ against pressure (fig. 23). Here, g is the acceleration of gravity, z height, c_p specific heat of air at constant pressure, T temperature, L latent heat of condensation, and q specific humidity. The parcel ascent is represented by a straight line on this diagram. At the surface (subscript zero) the potential energy is nil, so that $Q_o = (c_pT + Lq)_o$. Two parcel ascents, at the mean and extreme values of Q_o, have been entered in figure 23, together with the average distribution of Q against pressure for the period. These ascents terminate near 225 mb. and 150 mb., and this outlines the height range for the cumulonimbus anvils. There was no indication of strong variations in the mean sounding over the period which would have permitted the top of the convective layer to undergo large height changes. Therefore, the 150-mb. surface will be taken as the top of the tropospheric circulation cell. All integration with respect to pressure will be made from 1000 to 150 mb., neglecting the mass at pressures higher than 1000 mb. It should be noted that there is no requirement for $\bar{c}_n$ to vanish at 150 mb. as there may be stratospheric cells higher up; these cannot be analyzed, as the frequency of soundings diminished rapidly above 200-150 mb.

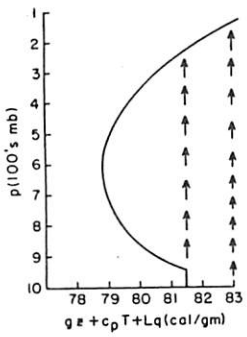

Figure 23. - Average distribution of total heat content in Gulf area during period as function of pressure. Arrows denote adiabatic ascent at mean and extreme heat content observed at surface.

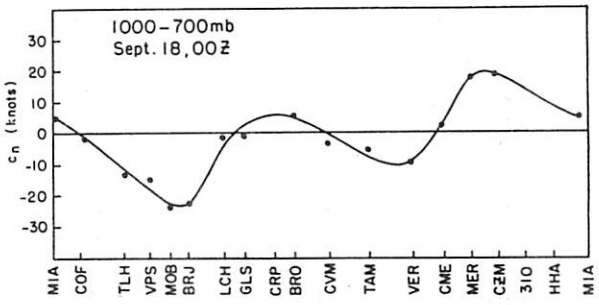

Figure 24. - Wind component normal to Gulf ellipse (knots) for layer 1000-700 mb., plotted as function of distance around Gulf, on Sept. 18, 1957, 0000 GMT.

The method one would like to use in computing $\bar{c}_n$ is to average c_n at all rawin stations for each reporting level and then to draw a curve of $\bar{c}_n$ so obtained against pressure. Unfortunately, this approach does not work. Since this study deals with daily and not time-averaged maps, details of the flow patterns must be taken into account, such as the jet streams in figures 12-14 which may be centered between observing stations. Further, there is a large gap in the rawins between Brownsville (BRO) and Merida (MER). Two more rawin stations are needed: at Tampico (TAM) and Vera Cruz (VER). If these were available, one could readily construct vertical cross sections of c_n around the ellipse, read c_n at evenly spaced grid points, and obtain mass balance with little need for adjustment. On account of the data gap, various techniques were tried out. The results shown in figures 25-26 were obtained as follows.

At first c_n was averaged with respect to pressure in layers of 100-mb. thickness (and over 50 mb. from 200 to 150 mb.) at all stations, including pilot balloon stations. To minimize the danger of including sea breeze effects, computations were made for the 0000 GMT (1800-1900 local time) observations. Where data were missing, however, soundings 6 and even 12 hours earlier or later were used. With these auxiliary winds and a few extrapolations to 10,000 feet, c_n was available for all stations on each day for the layer 1000-700 mb. This quantity was plotted on a diagram, with c_n as ordinate, and distance around the ellipse as abscissa. It is seen in figure 24 that a smooth curve can be fitted closely to all data points; from this curve the mass circulation in the layer 1000-700 mb. may be considered as well established.

Next, all values of c_n averaged over layers of 100-mb. thickness were

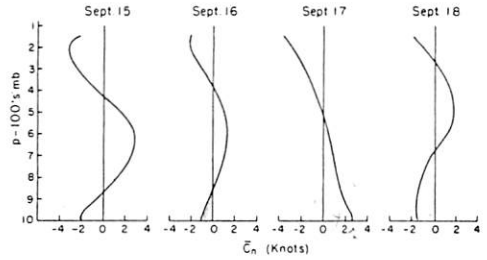

Figure 25. - Profiles of mean ageostrophic mass circulation $\bar{c}_n$ (knots).

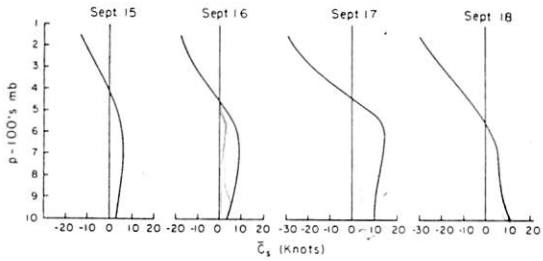

Figure 26. - Profiles of mean tangential component $\bar{c}_s$ (knots).

plotted and analyzed on cross sections with pressure on a linear scale as ordinate and distance around the ellipse as abscissa. Values were read at 20 evenly-spaced grid points in each layer from the analyses, and averaged. As expected, mass balance was not fully obtained. Adjustment of the analyses was then made in the data gap along the Mexican coast with qualitative aid from the upper-air charts. Undoubtedly, there remains an arbitrary element in the upper portions of the profiles of figure 25; the original aim to proceed on a purely numerical basis could not be carried through except for the layer 1000-700 mb. Quantitative procedures will become possible in the future if the number of upper-air stations continues to increase as in recent years; as stated initially, the present effort is only a first attempt. In spite of their shortcomings, the mass flow curves of figure 25 are considered to be sufficiently reliable to permit calculation of heat and energy fluxes through the ellipse.

According to figure 25, outflow of variable intensity took place in the high troposphere on all days, also inflow in the lower troposphere on the first three days, as is consistent with the picture of the thermal heat engine. A remarkable reversal followed on September 18 (see also fig. 24). The distribution of c_s (fig. 26) shows cyclonic circulation in low and middle troposphere and anticyclonic circulation, increasing with time, in the high troposphere.

4. BALANCE OF INTERNAL, POTENTIAL, AND LATENT HEAT ENERGY

Energy equations are treated in numerous textbooks. Therefore, no derivations will be offered here, only the final expressions used for calculation. The general equations contain all energy forms. As is well known, however, the terms containing kinetic energy are one or two orders of magnitude smaller than the other terms. Therefore, the energy balance will at first be computed, neglecting kinetic energy. Later a separate kinetic energy budget will be determined.

Assuming no vertical motion at 150 mb. and integrating over the boundary of the Gulf ellipse, the energy equation then takes the form

$$\frac{\partial}{\partial t}(I + P + M) = \iint (gz + c_p T + Lq)\, c_n ds \frac{dp}{g} + Q_e + Q_s + R \qquad (1)$$

Here, I. P. and M are internal, potential, and latent heat energy integrated over the ellipse; p is pressure, and t time. The heat source (S) within the ellipse

$$S = Q_e + Q_s + R \tag{2}$$

consists of latent (Q_e) and sensible (Q_s) heat exchange between air and ocean, and the net tropospheric radiation R. Equation (1) may be subdivided as follows:

$$\frac{\partial}{\partial t}(I + P) = \iint (c_p T + gz)\, c_n ds\, \frac{dp}{g} + Q_s + L\pi + R, \tag{3}$$

$$\frac{\partial M}{\partial t} = \iint Lq\, c_n d\, s\, \frac{dp}{g} + Q_e + L\pi, \tag{4}$$

where π is precipitation. Equation (4) permits separate determination of the moisture budget.

As shown in textbooks, $I + P = -p_T \tilde{z}_T A + c_p \int TdA \frac{dp}{g}$, where A denotes area, $\sim$ averaging with respect to area, and the integration is extended from the surface to the pressure surface p_T(top). The first term in this expression is negligible, so that I + P could be determined readily from thickness charts for the layer 1000-150 mb. Strictly, the dry temperature should be used, whereas the thickness is obtained from the virtual temperature. Since the total moisture was fairly constant through the period and only time derivatives are wanted for evaluating equations (1) - (4), use of thickness charts does not introduce appreciable error. The thickness and also the total moisture content were tabulated on a 22-point grid spread evenly over the interior of the ellipse and averaged. Then the integrated values were plotted against time, curves drawn, and the time derivative determined from the slope of the curves.

Transport terms: For the transport of $c_p T + gz$ and of Lq through the boundary, it was necessary to analyze these quantities on a vertical cross section around the Gulf just as in the case of the c_n component, and then read values from the analyses for the same grid points that were used to determine c_n. This proved a relatively easy task because Vera Cruz (VER) has a daily radiosonde observation, hence there was no large data gap on the western boundary of the ellipse. At first $c_p T + gz$ and Lq were averaged vertically over layers of 100-mb. thickness for each sounding, and then the mean of all ten radiosonde stations (Key West omitted) was computed for each layer to obtain $c_p \bar{T} + g\bar{z}$ and $L\bar{q}$. Stations were sufficiently evenly spaced that no further adjustment proved necessary. Then the deviations $(c_p T + gz)'$ and Lq' were computed at each station for each layer and plotted on cross sections. After analysis, the products $\overline{c_n'(c_p T + gz)'}$ and $\overline{c_n Lq'}$ yielded the

heat and moisture transport by the asymmetrical part of the circulation, the products $\bar{c}_n\ (c_p\bar{T} + g\bar{z})$ and $\bar{c}_n\ L\ \bar{q}$, the transports by the mean ageostrophic circulation.

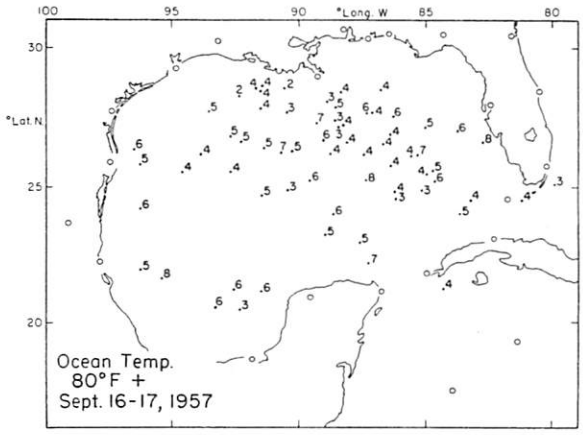

Figure 27. - Sea surface temperatures Sept. 16-17, 1957; departures from 80°F.

Heat sources and sinks: A mean daily cooling rate of 1°C./day was assumed for the net outgoing radiation, following previous calculations of the radiational heat loss in the Tropics. Day-to-day variations could not be assessed. Q_e was computed from the formula

$$Q_e = 1.71X10^{-6} L \int (q_w - q_a) V_o \, dA, \qquad (5)$$

where q_w and q_a are specific humidity at ocean surface and ship's deck level, and V_o is wind speed at ship's deck level. This formula, derived from the turbulence theory, has been applied, for instance, by the writer (Riehl et al. [9]) for calculation of the evaporation in the northeast trade of the Pacific Ocean. The formula has shortcomings which were discussed in the earlier paper and will not be reviewed here. The quantities q_w and q_a were obtained by plotting for the 4-day period, on 6-hourly charts, all dewpoints and sea surface temperatures reported by ships. Variations were irregular, so that finally all dewpoints and all sea surface temperatures were combined on one map each. Figure 27 contains the plot of the ocean temperatures. Variation appeared to be random, hence a single value for the mean surface temperature of the Gulf was computed; this amounted to 85°F., a very high value, which exceeded the seasonal mean by 2°F. Distribution of dewpoints was also irregular; the mean dewpoint temperature was 77°F. Because of the lack of determinable gradients in sea surface temperature and dewpoint, $(q_w - q_a)V_o$ in equation (5) may be replaced by $(\tilde{q}_w - \tilde{q}_a)\tilde{V}_o$. From the temperature data $\tilde{q}_w - \tilde{q}_a = 6.5$ g/kg, a large difference. V ranged from 5.1 m.p.s. on September 16 to 9.8 m.p.s. on September 18 when the tropical cyclone reached peak intensity. With these high winds and the large $\tilde{q}_w - \tilde{q}_a$ the evaporation was also large, ranging from 0.51 to 0.98 cm./day. Since the mean seasonal evaporation has been estimated near 0.5 cm./day, the first of these values is average, but the second value is exceptional and clearly related to the map situation. It is seen that large interdiurnal variations in heat source may be expected in the Tropics with varying synoptic conditions.

The sensible heat transfer Q_s, formerly considered to be a very small fraction of Q_e, has been assessed by Houghton [3] as 40 percent of Q_e for the annual heat balance of the globe. Riehl and Malkus [11] found that the same ratio holds for the equatorial trough zone alone. These estimates apply

only to averages over long periods and large areas. For want of better information, however, the ratio of 40 percent will be applied to the present Gulf case. Since Q_s depends on wind stirring and, following Riehl and Malkus [11], on the amount of cumulonimbus downdrafts, it is plausible that the sensible heat exchange between sea and air increased materially over the period analyzed.

With the assumptions and procedures as just discussed, the heat source was computed for each day, with results as given in table 1. To the extent that this table may be accepted as valid, large fluctuations in the heat source occurred, corresponding to progressive organization of the whole heat engine and development of the tropical storm.

Heat budget: Table 2 shows the heat energy budget determined from evaluation of all terms in equation (1); the residual imbalance is brought out through comparison of the local change of I + P + M determined from the curve and computed from advection and heat source. While there may be a systematic overvaluation of the source, the result as a whole appears fairly satisfactory. It must be remembered that rather crude methods had to be employed for evaluation of all terms; they may all contribute to the residual imbalance. The main result is that the net heat exchange through the boundary was nearly zero, so that the entire buildup of I + P + M over the Gulf took place by means of the local heat source.

Tables 3 and 4 show the budgets of M and of I + P separately. Of these, table 3 is considered most reliable because the moisture exchange takes place on the low levels. The moisture balance is hardly affected by errors in drawing the c_n-profiles in the upper troposphere. Therefore, all unbalance of table 2 has been placed into table 4.

The moisture budget contains the precipitation as residual that could not be measured. Because of the large size of the Gulf, one should expect only moderate precipitation depths in the mean over the whole area. This requirement is satisfied, as seen from the last column in table 3. It is of interest that the computed rainfall was highest on the two days when the cyclones were developing. Precipitation decreased sharply on September 16 when the first cyclone was entering land, and again on September 18 in spite of the tropical storm. This result may be attributed to the reversal of the whole circulation cell on that day (fig. 25), which led to subsidence and drying everywhere except in the immediate vicinity of the cyclone.

Table 3 shows that a strong moisture import took place through the boundary, accomplished mainly by the mean ageostrophic mass circulation. It is clear that without careful determination of this mass circulation it would be impossible to obtain a correct view of the energy transformations carried out by the heat engine over the Gulf. As already seen, the total heat flux through the boundary was nearly zero in the mean over the four days. Thus, the cell acts in part to convert imported latent heat to $gz + c_pT$, which must then be exported. This is confirmed by table 4, which also shows that transports due to ageostrophic mass circulation and due to asymmetries must be computed. One cannot assume the net mass circulation to be zero; nor can one

Table 1. – Heat sources and sinks (10^{14} cal./sec.).

Date (Sept. 1957)	$\tilde{V}_o$ m./s.	$\tilde{q}_w - \tilde{q}_a$ (g./kg.)	Evap. (cm./day)	Q_e	Q_s	Q_s+Q_e	R	Net heat source
15	6.2	6.5	.62	.68	.27	.95	-.38	.57
16	5.1	6.5	.51	.56	.22	.78	-.38	.40
17	7.0	6.5	.70	.77	.31	1.08	-.38	.70
18	9.8	6.5	.98	1.08	.43	1.51	-.38	1.13

Table 2. – Heat energy budget (10^{14} cal./sec.) (evaluation of equation (1)).

Date (Sept. 1957)	$\frac{\partial}{\partial t}(I + P + M)$ from curve	$\frac{\partial}{\partial t}(I + P + M)$ from right side	= Advection	+ Source
15	.74	.91	.34	.57
16	-.19	-.34	-.74	.40
17	.45	.87	.17	.70
18	.66	1.33	.20	1.13
Total 15-18	1.66	2.77	-.03	2.80

Table 3. – Latent heat energy budget (10^{14} cal./sec.).

Date (Sept.)	Local change (from curve)	= Advection by mass circ.	+ Advection by Asymmetries	+ Q_e	- $L\pi$ (residual)	Precip. cm./day
15	.34	.29	.60	.68	-1.23	1.10
16	-.19	.12	-.34	.56	- .54	.49
17	.14	.97	.08	.77	-1.68	1.50
18	-.14	-.26	.13	1.08	-1.09	.99
Total 15-18	.15	1.12	.47	3.09	-4.54	1.02

Table 4. – Budget of $c_pT + g\,z$ (10^{14} cal./sec.).

Date (Sept.)	$\frac{\partial}{\partial t}(I+P)$ from curve	$\frac{\partial}{\partial t}(I+P)$ from right side	= Advection by mass circ.	+ Advection by Asymmetries	+ R	+ Q_s	+ $L\pi$
15	.40	.57	- .70	.15	- .38	.27	1.23
16	0	-.15	- .32	-.20	- .38	.22	.53
17	.31	.73	-1.14	.26	- .38	.31	1.68
18	.80	1.47	.33	0	- .38	.43	1.09
Total 15-18	1.51	2.62	-1.83	.21	-1.52	1.23	4.54

***If Q_s had been computed with the classical method, the difference between $(\partial/\partial t)(I+P)$ from the curve and from the right side of the table would be materially reduced.**

make the assumption of horizontally uniform temperature and moisture, in spite of the relative homogeneity of the tropical air mass.

Table 4 indicates further that a small part of the precipitation is used to balance the excess of R over Q_s; that a large part is used for the sensible heat export as just mentioned; and, that all increase in I + P results from precipitation heating when the change over the four days is considered. With this, a quantitative demonstration of part of the simple heat engine has been given. For an estimate of conversion of latent heat released to kinetic energy through building up the potential energy over the Gulf, we now turn to the kinetic energy budget.

5. BUDGET OF KINETIC ENERGY

If the kinetic energy equation per unit mass is integrated over the mass inside the ellipse, one obtains, neglecting vertical kinetic energy,

$$\frac{\partial K}{\partial t} = \frac{1}{2}\int_p\int_s V^2 c_n ds\frac{dp}{g} - \int_p\int_A \mathbb{V}\cdot\nabla h dA dp + \int_p\int_A \mathbb{V}\cdot\mathbb{F}\, dA\frac{dp}{g} \qquad (6)$$

Here, K is the integrated kinetic energy of the mass inside the ellipse, V scalar wind speed, $\mathbb{V}$ vector wind, and ∇ the two-dimensional gradient operator. For calculation of local change and transport terms, the techniques already outlined for the heat energy budget were applied, except that determination of K was made from isotach analyses at six levels. There was much leeway in drawing the lines in the middle troposphere, where the change from lower to upper circulation occurred. This proved to be without importance, because most kinetic energy was concentrated in the two jet streams and the tropical storm, all of which could be described with fair certainty.

Evaluation of the production of kinetic energy by pressure forces could not be fully carried out because knowledge of the three-dimensional distribution of $\mathbb{V}\cdot\nabla h$ is required. Only a partial computation can be made after the following transformations (cf. Starr [13]). We can write

$$-\iint \mathbb{V}\cdot\nabla h dA dp = -\iint \nabla\cdot(\mathbb{V}h)\, dA dp + \iint h\nabla\cdot\mathbb{V}\, dA dp.$$

Now $-\iint \nabla\cdot(\mathbb{V}h)\, dA dp = -\int hc_n ds dp = -s\int \bar{h}\,\bar{c}_n dp - s\int \overline{h'c_n'}dp.$

This term represents the work done by pressure forces through the ellipse. Nearly all of this was accomplished by the mass circulation, so that the $\overline{h'c_n'}$ term can be neglected as a secondary effect.

The term $\iint h\nabla\cdot\mathbb{V}\, dA dp = A\int \tilde{h}\,\widetilde{\nabla\cdot\mathbb{V}}\, dp + \iint \widetilde{h'\,\nabla\cdot\mathbb{V}'}\, dA dp.$ since $\widetilde{\nabla\cdot\mathbb{V}} = \frac{1}{A}\int c_n ds$, $A\int \tilde{h}\,\widetilde{\nabla\cdot\mathbb{V}}\, dp = s\int \tilde{h}\,\bar{c}_n dp$. The production term can now be written

$$-\iint \mathbb{V}\cdot\nabla h dA dp = s\int(\tilde{h}-\bar{h})\,\bar{c}_n dp + \iint \widetilde{h'\,\nabla\cdot\mathbb{V}'} dA dp \qquad (7)$$

In this formula the first term on the right-hand side can be determined from the ellipse boundary data and the constant pressure charts. It measures the production of kinetic energy by the mass circulation acting on the mean pressure difference between boundary and interior. With inflow toward lower pressure near the ground and outflow from the upper anticyclone also toward lower pressure at high levels, this term will make a positive contribution to kinetic energy generation. The second term essentially measures the production that arises, for instance, from the penetration of the flow toward small areas of particularly low pressure within the general envelope during convergence. From the well known association between convergence

and vorticity, and hence indirectly with the pressure field through the gradient wind equation, we must assume that this term will be large and may be dominant. Variations in the efficiency of the thermal heat engine in converting latent heat to kinetic energy will depend largely on the role played by this term. Highest efficiency evidently will be attained in hurricanes, where most inflowing mass penetrates to a local area of very low pressures before converging and ascending. It is this important term that cannot be computed from the ellipse data and must be treated as residual.

The frictional force per unit mass $\mathbf{F} = \frac{1}{\rho}\frac{\partial \boldsymbol{\tau}}{\partial z}$, where $\boldsymbol{\tau}$ is the shearing stress vector. Therefore the frictional dissipation of kinetic energy

$$\int \mathbf{V} \cdot \mathbf{F}\, dA\, \frac{dp}{g} = \int_{\alpha} \mathbf{V} \cdot \frac{\partial \boldsymbol{\tau}}{\partial z} d\alpha = \int_{\alpha} \frac{\partial}{\partial z} \mathbf{V} \cdot \boldsymbol{\tau}\, d\alpha - \int_{\alpha} \boldsymbol{\tau} \cdot \frac{\partial \mathbf{V}}{\partial z}\, d\alpha.$$

where α denotes volume. The first of the terms on the right-hand side gives the dissipation at upper and lower boundaries, the second the internal dissipation within the atmosphere (cf. Palmén and Riehl [5]). Dissipation at the top is presumably negligible. Therefore we obtain

$$\int_{\alpha} \frac{\partial}{\partial z} \mathbf{V} \cdot \boldsymbol{\tau}\, d\alpha = -\int_{A} (\mathbf{V} \cdot \boldsymbol{\tau})_o\, dA \qquad (8)$$

after integration. Further, $\boldsymbol{\tau}_o$ may be expressed through the well known formula $\boldsymbol{\tau}_o = k\rho_o \mathbf{V}_o V_o$, where $\mathbf{V}_o$ is the vector wind at ship's deck level, ρ_o the density of the air at the surface, and k an aerodynamic constant. Then $-\int (\mathbf{V} \cdot \boldsymbol{\tau})_o dA = -k\, \rho_o V_o^3\, A$. This term can be computed because fairly reliable isotachs could be drawn over the water from ship observations. We shall assume that the surface stress is 1 dyn./cm.^{2} at normal trade wind speeds of 7 m.p.s. Given $\rho_o = 1.2 \times 10^{-3}$ g./cm.^{3}, k = 0.0017. Excepting a small area around the center of the tropical storm, wind speeds did not vary enough over the period analyzed to require consideration of variations of k with V_o on account of changes in surface roughness.

Very little is known about the internal dissipation of kinetic energy. We shall assume, following Brunt [2] and Palmén [6], that it does not exceed the dissipation due to ground friction. Certainly we should expect that, as the surface winds and vertical shears increased over the period studied, the internal dissipation also increased. While the results of computations made with the foregoing assumptions will necessarily be rough, it is nevertheless believed that the relative importance of all terms in the kinetic energy budget and their variations with time are fairly well represented in table 5.

According to the table, the total kinetic energy continually rose over the four days. At first the increase was concentrated at high levels, leading to development of the jet streams; later in the low troposphere during the

Table 5. – Kinetic energy budget (10^{12} cal./sec.).

Date (Sept.)	$\frac{\partial k}{\partial t}$	=	Import	+ Production by mass circ.	+ Production by $h'\nabla \cdot \overline{V}$ (residual)	– Dissipation by friction (ground plus internal)	Efficiency of heat engine (%)	Total kinetic energy (10^{16} cal.)	Dissipation by friction 10^{16} cal./day	Export by mass circ.	Export by asymmetries
15	.37		- .13	.50	.44	- .44	0.8	7.1	3.8	-.07	- .06
16	.48		- .35	.42	.71	- .30	2.1	11.1	2.6	-.09	- .26
17	.48		-1.52	1.70	1.18	- .88	1.7	15.4	7.6	-.24	-1.28
18	.37		-2.02	-.35	4.88	-2.14	4.1	19.1	18.5	-.07	-1.95
Total 15-18	1.70		-4.02	2.27	7.21	-3.76					

tropical storm development. Altogether, the kinetic energy nearly tripled during the period. This increase was overshadowed by a large export of kinetic energy, concentrated in the two jet streams on September 17 and 18. Export by the asymmetric part of the circulation - the jet streams - predominates strongly over export by the mass circulation (right-hand side of table 5). It is clear that for computation of a kinetic energy budget, symmetrical models cannot be used.

The rate of frictional dissipation rose by almost an order of magnitude during development of the tropical storm and the jet streams to attain values comparable with those computed by Palmen and Riehl [5] for a fully mature hurricane (3.6×10^{12} cal./sec. for the ground friction term for a comparable area). In this situation, as in other tropical storm cases, large frictional dissipation at the ground arose from the fact that winds of moderate intensity were spread over a large area, whereas in hurricanes, very strong winds cover a small core. On the first three days (cf. table 5) the dissipation rate per day was one-half to one-third of the total kinetic energy in the air over the Gulf; on the last day the dissipation per 24 hours approximately equalled the total kinetic energy; this also corresponds to Palmen and Jordan's [4] findings in hurricanes. Thus, though no hurricane developed, the picture is quite comparable as far as dissipation is concerned.

This must be true also for production of kinetic energy. In Palmen's computation there was no kinetic energy export through the hurricane boundary;

in the present situation there was a large export, roughly equalling the frictional dissipation. Therefore the production term is large on all four days, and on September 18 Palmén's value of 3.6×10^{12} cal./sec. is exceeded. Nevertheless, no hurricane formed, as the excess kinetic energy produced was largely exported. On the first three days production by the mass circulation was important and equal to the $\widetilde{h' \nabla \cdot \mathbb{V}'}$ term, especially on September 17. A marked difference occurred on the 18th. With the reversal of mass circulation the whole cell tended to become "indirect," consuming rather than releasing kinetic energy. All production became localized in the tropical storm. Table 5 contains a column showing the efficiency of the thermal heat engine, defined here as the ratio of kinetic energy produced to latent heat released through condensation. On the first three days the efficiency was 1 to 2 percent, in accordance with usual estimates; it rose to 4 percent on the 18th, according to the table. If this figure is reliable, it denotes that the ascending portion of the mass circulation became entirely concentrated in the tropical storm, whereas there was widespread ascent on the 17th.

6. COMPARISON OF THE CYCLONE OF SEPTEMBER 17-18 AND HURRICANE AUDREY

As evident from table 5, the event analyzed was of large magnitude as far as kinetic energy production in secondary circulations of the Tropics is concerned. The question may be raised why the tropical storm, after a good start, failed to become a hurricane. This question cannot be answered fully, because the sufficient conditions for hurricane formation are not known. Some suggestions, however, are contained in the foregoing material. Moreover, analysis was made for the development period of hurricane Audrey (June 24-27, 1957) in the Gulf, similar to that just described. On June 24 the situation over the Gulf resembled that of September 16, except that a stronger belt of easterlies covered the northern Gulf coast; motion of the cyclone in the southwestern Gulf also was appreciably slower. The low-level maps of June 25, 0000 GMT were almost identical with those of September 17, 0000 GMT, but development during the next 24 hours differed greatly. While two cases obviously do not suffice for definite conclusions about the trigger mechanism for cyclogenesis, it will nevertheless be of interest to determine the differences between the two situations.

One may ask whether calculations performed for the whole ellipse can be applied readily to a tropical storm centered in the western Gulf and moving northward. For determination of the mass circulation relative to the tropical storm in September, only ship winds and a few low-level reconnaissance winds are available. An attempt was made to determine the mass circulation by plotting all reports within six hours of the 0000 GMT map times on September 17 and 18 on one chart, positioned with respect to the center. The preceding 1200 GMT maps were also used to help fill in areas without reports. Results were necessarily rough. Nevertheless, profiles of the mass circulation could be determined for the outskirts of the center (fig. 28); near the core reports were too few to permit calculation. The ellipse computation does not satisfy the geometrical requirements for radial velocity, but surface values from figure 25 have been entered in figure 28 at the mean radius of the Gulf, which is 7° of latitude.

It is seen that the ellipse data are not contradicted by the ship observations, and by the shift of coordinates to a polar coordinate system fixed in the tropical storm. On September 17 inflow and convergence took place around the whole periphery of the center, while on September 18 divergence prevailed over the whole calculable portion of the v_r-profile, with actual outflow beyond the 6° radius. Comparison with the mass circulation of the mean hurricane (Palmén and Riehl [5]), also shown in figure 28, indicates that the change in mass circulation from September 17 to 18 may have had a decisive effect on the storm.

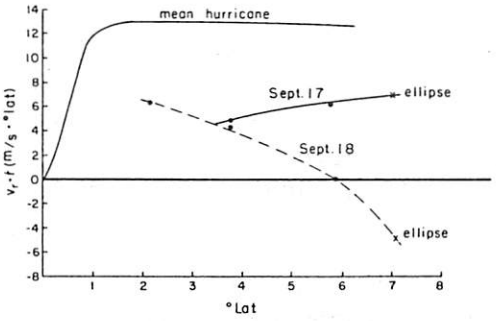

Figure 28. - Distribution of mass circulation ($v_r \cdot r$) at surface against radius (°lat.) in coordinate system centered on tropical storm for Sept. 17 and 18. Ellipse values and profile of mass circulation for mean hurricane are also shown.

This suggestion is also supported by the hurricane Audrey data. Quantitative comparison of the two cases is possible by considering the transport of absolute vorticity through the ellipse boundary. The vorticity equation, neglecting friction, tilting terms, and vertical vorticity transport, may be written

$$\frac{\partial \zeta}{\partial t} + \nabla \cdot \mathbb{V}\zeta = 0, \tag{9}$$

where ζ is the absolute vorticity. Integrating over the Gulf between isobaric surfaces,

$$\int \frac{\partial \zeta}{\partial t} \, dA \, \frac{dp}{g} = \frac{\partial}{\partial t} \int c_s ds \, \frac{dp}{g} = - \int \zeta c_n ds \, \frac{dp}{g} ,$$

or

$$\frac{\partial}{\partial t} \int \overline{c}_s dp = - \int \overline{\zeta c_n} \, dp = - \int (f + \zeta_r) \, c_n \, dp , \tag{10}$$

where f is the Coriolis parameter and ζ_r the relative vorticity. In the form of the vorticity equation the quantity ultimately of interest in hurricane prediction, $\frac{\partial \overline{c_s}}{\partial t}$, appears explicitly. In view of the restricted form of equation (9), application of equation (10) should be made only to changes of $\frac{\partial \overline{c_s}}{\partial t}$ integrated over deep layers of the troposphere. When used in this way, good results were obtained. One would prefer to evaluate the equation for layers of 100-mb. thickness. This did not prove feasible, presumably on account of strong vertical vorticity advection. Nevertheless, it is of

interest to discuss the vertical distribution of $\overline{\zeta c_n}$. On September 17, the calculation predicted an increase of $\overline{c_s}$ of 3.5 knots/24 hours for the layer 1000-600 mb. and a decrease of 4 knots/24 hours for the layer 600-200 mb., with level of nondivergence at 600 mb. The same level of nondivergence was found on June 25, but on this occasion the calculated changes of $\overline{c_s}$ were +18 knots/24 hours for the lower troposphere and -10 knots/24 hours for the upper troposphere. There was, then, a large difference in the intensity of the acceleration of circulation as produced by convergence around the Gulf, in spite of the superficial resemblance of the charts. In addition, a distribution of low-level inflow and high-level outflow through the ellipse continued on June 26 and 27, though much weaker than on June 25. There was no reversal as on September 18.

In other respects both situations were quite comparable. The total heat flux through the boundary was small. Internal energy and total moisture actually were a little lower in the June than in the September case. The evaporation also was stronger in September, at least prior to establishment of hurricane Audrey. Dewpoints averaged near 77° F. in both cases, but the sea surface temperature was 85° F. in September compared to 83° F. in June; thus, the difference $\tilde{q}_w - \tilde{q}_a$ was 6.5 g./kg. in September and 5 g./kg. in June, rendering the September situation more favorable from the ocean temperature viewpoint.

It follows that the only evident difference of importance between the two cases lay in the mechanical concentration of vorticity $\overline{c_n \zeta}$, and this difference was brought about by an entirely different evolution of the flow over the United States. Riehl [7] has pointed out that hurricane formation is likely to occur when an upper-air trough of large amplitude in the north, propagating eastward, passes a well-developed wave in the easterlies or equatorial shear line with incipient vortex. Principal deepening occurs after the middle-latitude trough has moved well to the east of the tropical disturbance and fracture of the two systems is taking place. Exactly this sequence of events happened on June 24-26, with fracture occurring early on June 25. In contrast, no trough passage was observed during September 16-18 (figs. 11-13); southwesterly winds persisted north of the Gulf coast.

On account of lack of sufficient data it has never been possible to compute the mechanism by which eastward passage of a trough in the north influences an incipient tropical storm far to the south. From the details of the c_n distribution around the Gulf in the Audrey situation it can be seen that a strong injection of air into the Gulf in low and middle troposphere took place to the rear of the upper trough across a large portion of the northern Gulf coast. This fresh inflow, coupled with preexisting inflow from the south into the tropical disturbance, led to the strong net inflow in the low troposphere (4 knots) and to the resulting high values of $\overline{\zeta c_n}$.

7. CONCLUSION

The preceding comparison of the tropical cyclone situations of June and September 1957 leads to the hypothesis that mechanical forcing from neighboring disturbances is an important factor in the deepening of tropical disturbances to hurricane strength. It will be necessary to test this hypothesis in a large number of cases to ascertain its validity. Even if successful, an ultimate understanding of the hurricane would not be obtained. For, since gradient wind balance is closely fulfilled in tropical storms, it is necessary to arrive at an understanding of the pressure gradient requisite to maintain the c_s field calculated from the vorticity equation under gradient wind conditions. This problem cannot be solved with observations as utilized in this report, but may be attacked with research aircraft missions into storm centers as flown by the National Hurricane Research Project of the U. S. Weather Bureau.

This study has shown that thermally direct circulations which produce and export large amounts of kinetic energy can occur in the Tropics even without a hurricane or typhoon. In fact, it has been seen that existence of a direct cell is not a sufficient condition for deepening of a tropical disturbance. It will be of interest in subsequent work to determine the frequency of such systems and their contribution toward maintaining the general circulation. Further, it will be necessary to investigate the circumstances that permit their development and control the duration of their existence.

ACKNOWLEDGMENTS

This report was prepared under a contract between the Office of Naval Research, U. S. Navy, and The University of Chicago. All observations and charts used during the research were furnished by the National Hurricane Research Project through the courtesy of its director, Mr. R. H. Simpson.

REFERENCES

1. R. R. Braham, "The Water and Energy Budgets of the Thunderstorm and Their Relation to Thunderstorm Development," Journal of Meteorology, vol. 9, No. 4, Aug. 1952, pp. 227-242.
2. D. Brunt, Physical and Dynamical Meteorology, 2d Ed., The University Press, Cambridge, 428 pp., 1939.
3. H. G. Houghton, "On Annual Heat Balance of the Northern Hemisphere," Journal of Meteorology, vol. 11, No. 1, Feb. 1954, pp. 1-9.
4. E. Palmén and C. L. Jordan, "Note on the Release of Kinetic Energy in Tropical Cyclones," Tellus, vol. 7, No. 2, May 1955, pp. 186-188.
5. E. Palmén and H. Riehl, "Budget of Angular Momentum and Energy in Tropical Cyclones," Journal of Meteorology, vol. 14, No. 2, Apr. 1957, pp. 150-159.
6. E. Palmén, "Vertical Circulation and Release of Kinetic Energy During the Development of Hurricane Hazel as an Extratropical Storm," Tellus, vol. 10, No. 1, Feb. 1958, pp. 1-24.
7. H. Riehl, "On the Formation of West-Atlantic Hurricanes," Department of Meteorology, The University of Chicago, Miscellaneous Report No.24, Part I, 102 pp.

8. H. Riehl and N. M. Burgner, "Further Studies of the Movement and Formation of Hurricanes and their Forecasting," Bulletin of the American Meteorological Society, vol. 31, No. 7, Sept. 1950, pp. 244-253.
9. H. Riehl et al.,"The Northeast Trade of the Pacific Ocean," Quarterly Journal of the Royal Meteorological Society, vol. 77, No. 334, Oct. 1951, pp. 598-626.
10. H. Riehl, Tropical Meteorology, McGraw-Hill Book Co., Inc., New York, 392 pp., 1954.
11. H. Riehl and J. S. Malkus, 1958: "On the Heat Balance in the Equatorial Trough Zone. Palmén 60th anniversary volume (complete reference will be available later in year).
12. R. H. Simpson, "Synoptic Aspects of the Intertropical Convergence near Central and South America," Bulletin of the American Meteorological Society, vol. 28, No. 7, Sept. 1947, pp. 335-346.
13. V. P. Starr,"Applications of Energy Principles to the General Circulation," Compendium of Meteorology, T. F. Malone, ed., American Meteorological Society, Boston, pp. 568-574.